THE JOURNAL OF PHYSICAL CHEMISTRY B
A JOURNAL OF THE AMERICAN CHEMICAL SOCIETY

pubs.acs.org/JPCB

Article

Step-Wise Hydration of Magnesium by Four Water Molecules Precedes Phosphate Release in a Myosin Motor

Published as part of The Journal of Physical Chemistry virtual special issue "Lawrence R. Pratt Festschrift".

Mauro Lorenzo Mugnai and D. Thirumalai*

Cite This: *J. Phys. Chem. B* 2021, 125, 1107–1117

Read Online

ACCESS | Metrics & More | Article Recommendations | Supporting Information

ABSTRACT: Molecular motors, such as myosin, kinesin, and dynein, convert the energy released by the hydrolysis of ATP into mechanical work, thus allowing them to undergo directional motion on cytoskeletal tracks. A pivotal step in the chemomechanical transduction in myosin motors occurs after they bind to the actin filament, which triggers the release of phosphate (P_i, product of ATP hydrolysis) and the rotation of the lever arm. Here, we investigate the mechanism of phosphate release in myosin VI using extensive molecular dynamics simulations involving multiple trajectories of several μs. Because the escape of phosphate is expected to occur on time-scales on the order of milliseconds or more in myosin VI, we observed P_i release only if the trajectories were initiated with a rotated phosphate inside the nucleotide binding pocket. We discovered that although P_i populates the traditional "back door" route, phosphate exits through various other gateways, thus establishing the heterogeneity in the escape routes. Remarkably, we observed that the release of phosphate is preceded by a stepwise hydration of the ADP-bound magnesium ion. The release of the anion occurred only after four water molecules hydrated the cation (Mg^{2+}). By performing comparative structural analyses, we show that hydration of magnesium is the key step in the phosphate release in a number of ATPases and GTPases. Nature may have evolved hydration of Mg^{2+} as a general molecular switch for P_i release, which is a universal step in the catalytic cycle of many machines that share little sequence or structural similarity.

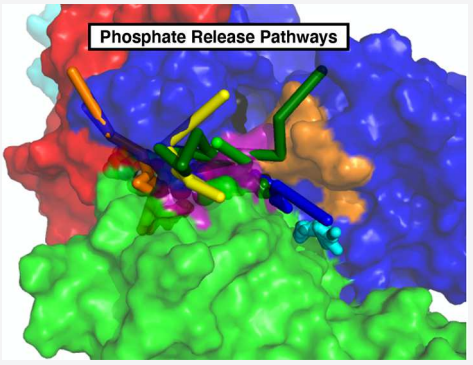

INTRODUCTION

Myosins are molecular motors that, fueled by the hydrolysis of ATP, move unidirectionally on a cytoskeletal track (the filamentous actin, or F-actin).[1,2] To perform their functions, myosins, like other motors, undergo a chemomechanical cycle in which the nature of the nucleotide bound to the enzyme [no nucleotide (apo), ATP, ADP and P_i, and ADP] is coupled with the three-dimensional structure attained by the myosin head, and with nucleotide-dependent affinity for actin (Figure 1a). After catalyzing the hydrolysis of ATP, myosin binds to the filament; this triggers the release of phosphate and the "power-stroke," a conformational transition in which the movement of the converter domain (black in Figure 1a) is amplified by the rotation of the lever arm (cyan in Figure 1a, where only a small fragment of the full lever arm is shown). While myosin ADP-bound and apo states are tightly bound to actin, the binding of ATP induces the dissociation of the actomyosin complex. Finally, the hydrolysis of ATP is coupled to the "re-priming" stroke, a transition during which the lever resumes the pre-power-stroke (PrePS) conformation, thereby preparing myosin for a new cycle.

The pivotal step of the chemomechanical transduction is the power stroke, which occurs when myosin binds to the actin filament after ATP hydrolysis. The interaction between the motor and the track is believed to stabilize a conformation that accelerates phosphate release (see De La Cruz et al.[3] for myosin VI) and produces the forward swing of the lever arm. To elucidate the details of this crucial step in the myosin catalytic cycle, it is therefore necessary to achieve a detailed molecular-level understanding of the processes governing phosphate release, which is possible using atomically detailed molecular dynamics simulations.

When the first structure of a myosin bound to ADP and an analog of P_i was resolved,[4] the release pathway of P_i immediately posed a puzzle. ATP binds the motor domain with the γ-phosphate buried inside the nucleotide binding site. As a consequence, it is possible that ADP hinders the release of P_i from the entrance gateway, suggesting that an alternative exit route must exist. Yount et al. postulated that there is a "back door" pathway for the release of P_i along the seam that

Received: November 5, 2020
Revised: January 11, 2021
Published: January 22, 2021

https://dx.doi.org/10.1021/acs.jpcb.0c10004
J. Phys. Chem. B 2021, 125, 1107–1117

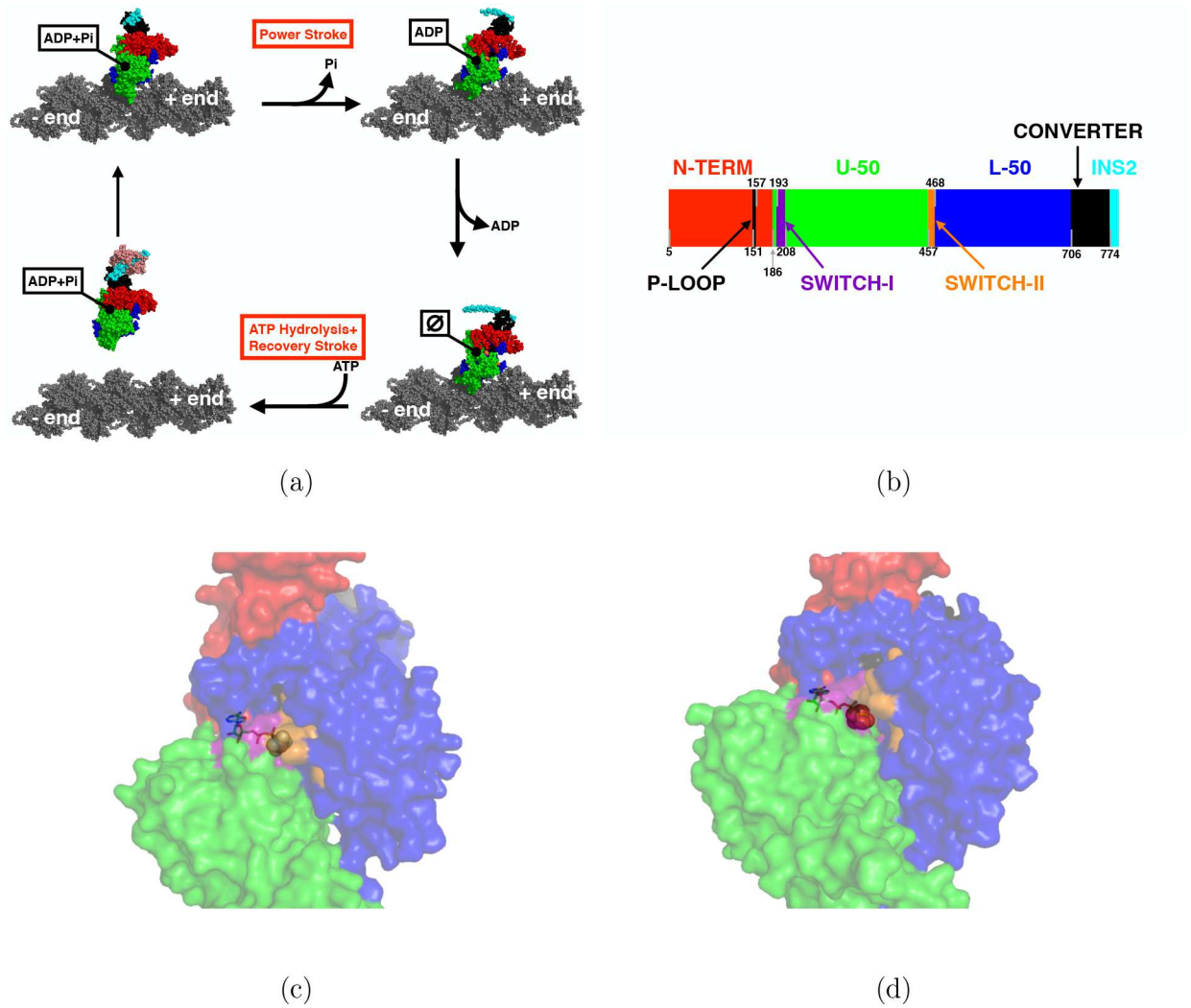

Figure 1. Sequence, cycle, and structure of myosin VI. (a) Myosin cycle. The different conformations are taken from a combination of structural studies: actin and ADP-bound myosin (top right) (PDB 6BNW[10]), actin and rigor (or apo, bottom right) (6BNV[10]), pre-power stroke (ADP+P_i, detached from actin, bottom left) (4ANJ,[11] crystallized with a phosphate analog), and phosphate release (P_iR, ADP-P_i, attached to actin, top left) (4PJM[6]). The ADP-bound and rigor states were solved in the presence of actin; the P_iR myosin was aligned to the ADP-bound myosin. (b) Sequence of myosin VI. The color code for representing the different structural elements is kept throughout the paper. The identification of individual elements follows indications from multiple sources.[1,2,6] However, we do not show some groups that we do not discuss in the paper (for instance, the relay helix) and the domains that we consider do not correspond precisely to the proteolytic fragments.[1] (c) Filled-mode representation of myosin VI in PrePS (PDB 4ANJ[11]). ADP and P_i are shown as sticks and can be seen through the transparent motor. The "back door" pathway is closed in the PrePS conformation (see the purple orange shades showing Switch-I and -II). (d) P_iR conformation is represented in filled mode, with the ligands shown as sticks (PDB 4PJM[6]). The "back door" pathway is now open: the purple and orange shades (Switch-I and -II) have moved away from each other and the phosphate is more clearly visible.

separates the so-called U-50 and L-50 domains of the motor[5] (see Figure 1a,b). Although such a release route appears to be open when the nucleotides are missing from the binding site, in the PrePS conformation, crystallized with ADP and an analog of P_i bound to myosin, this route is closed by two loops, Switch-I and Switch-II (Figure 1c). Thus, either or both of the loops must move to open the "back door" channel, although such displacements are also expected to reduce the efficiency of the motor.[6] A solution to this puzzle emerged when the crystal structure of a myosin in a putative P_i-release (P_iR) conformation was resolved.[6] The structure shows partial movement of Switch-II, which opens the "back door" pathway (Figure 1d), and a change in the actin-binding interface that was suggested to strengthen the interaction with F-actin.[6] In addition, the converter is found in pre-stroke position, indicating that P_i release precedes the power stroke, and a combination of kinetics and structural experiments supported the interpretation of this structure as the P_iR conformation.[6] These findings are in agreement with optical trap experiments for myosin V,[7] although at odds with experiments in muscle fibers[8] and ultrafast force clamp measurements[9] that identified the existence of a force-generating state prior to phosphate release.

It is important to point out that the putative P_iR structure was solved in the absence of actin. Whether this conformation is the one that is stabilized by the interaction with the filament, and whether it constitutes an on-pathway phosphate-release intermediate, has yet to be fully established. The most direct way to test this hypothesis would be to solve the P_iR state complexed with actin using cryo-EM. High-resolution

https://dx.doi.org/10.1021/acs.jpcb.0c10004
J. Phys. Chem. B 2021, 125, 1107−1117

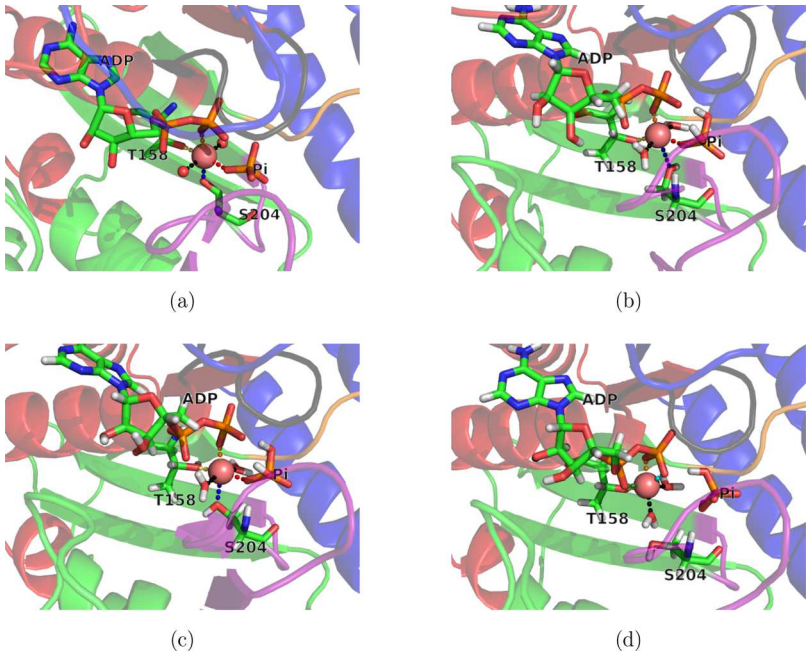

Figure 2. Coordination of Mg^{2+} after equilibration. (a) In the crystal structure (4PJM), Mg^{2+} ion is coordinated by two water molecules (shown as spheres), T158, S204, Pi, and one oxygen from ADP β-phosphate. (b) Conformation of the nucleotide binding site after equilibration starting with the CA initial conformation. Similarly to the crystal structure in panel a, the first shell of Mg^{2+} is occupied by T158, S204, P_i, and one oxygen from ADP β-phosphate. (c) Initial structure for the simulations carried out with the $Mg_{(ANV)}{}^{2+}$ divalent cation. The coordination shell of Mg^{2+} is not affected by the choice of the force field. (d) Nucleotide binding pocket of MVI after equilibration with the P_i rotated to point a hydroxyl group toward Mg^{2+} (RA initial conformation). Distortion induced by the different orientation of the P_i modifies the first shell of Mg^{2+}, which is now made by two water molecules, three oxygens from ADP diphosphate, and T158.

structures in tight-binding states (ADP-bound and rigor) have recently been obtained for myosin VI.[10] However, if the weak-to-strong transition follows the release of phosphate,[6] the weakly bound P_iR-actin complex might be difficult to characterize. In the context of this work, we assume that this is the intermediate stabilized by actin, but future studies will be necessary to ascertain this critical point.

Although it appears that the "back door" pathway for P_i release is open in the P_iR conformation, this might not be the unique exit route for P_i, as suggested by computational studies adopting enhanced sampling techniques.[12] Furthermore, a clear picture of the microscopic conformational transitions leading to the P_i release is lacking. In particular, the role that water molecules (which hydrate the cation, see Figure 2a) play in enabling P_i release has not been probed. To remedy this situation, we investigate the mechanism of P_i release from myosin VI (MVI) nucleotide binding site by running many multimicrosecond molecular dynamics (MD) trajectories generated using the supercomputer Anton 2.[13] Experimentally, the actin-activated average P_i release time from the PrePS conformation is expected to be in the range from 8.3 ms−33 ms,[3,14,15] which is still beyond the current computational capabilities for conventional all-atom MD simulations of systems as large as myosin (although enhanced sampling methods,[12,16] and spatial[17] or temporal[18] coarse-graining have allowed to access longer time scales). Accordingly, we only observed the release of phosphate within the time scale accessible to Anton 2 when the simulations were started with a rotated P_i, which we believe is sufficient to reveal the complexities of P_i release. This perturbation weakens the interaction between the phosphate and the ADP-bound Mg^{2+} because a P_i hydroxyl group (instead of an oxygen of P_i) is placed in the coordination shell of the cation. In what follows, we refer to "CA" (crystallographically aligned) as the initial conformation attained by ensuring that a phosphate oxygen group points toward the magnesium ion (see Figure 2b,c); we term instead "RA" (rotated alignment) the structure in which the phosphate is initially rotated (see Figure 2d).

Strikingly, we found that water molecules play a crucial role in the escape of phosphate. First, we observed that the magnesium cation is progressively hydrated in a stepwise manner. Second, in all the simulations resulting in the release of phosphate, before the P_i leaves the proximity of ADP, four water molecules hydrate the magnesium, upward from the two found in the crystal structure. This leads us to suggest that the hydration of magnesium by four discrete water molecules, which serves as a switch, is the step that triggers the release of phosphate. By comparing the structures of the nucleotide binding pockets in other biological machines, we believe that this important discovery might constitute a general mechanism for phosphate release in many families of ATPases and GTPases (for instance myosins, kinesins, and G-proteins[19]). We show that these machines share similar structural features in their nucleotide binding sites. Thus, we have discovered using computations a unifying mechanism of P_i release in a class of biological machines. Our findings are amenable to experimental tests.

METHODS

Crystal Structure. We started from the crystal structure in PDB 4PJM,[6] which was obtained after soaking the crystal in a phosphate bath. The structure indicates that the P_i and a few residues are found in two alternative conformations labeled A and B. The simulations employed conformation B, in which the P_i and R136 (at the interface between N-terminal region

https://dx.doi.org/10.1021/acs.jpcb.0c10004
J. Phys. Chem. B 2021, 125, 1107−1117

and the converter) are closer to the spatial arrangement of P_i in structure 4PFP. In addition, the hydrogen bond between S153 and P_i, which is formed in structure 4PFP, is broken if the B conformation of S153 is chosen. This likely weakens the phosphate interaction in the nucleotide binding site and may facilitate its release. The water molecules identified in the crystal structure were maintained as a part of the model. In the crystal structure 4PJM, four segments of the myosin motor were not resolved (175−179, 397−406, 565−566, 623−637). We modeled them using Swiss-PDB Viewer.[20] Because they are far from the nucleotide binding site, it is unlikely that their precise structure significantly affects the release of P_i. To establish the protonation state of the histidines, we used ProPKa.[21,22]

Force Fields. The simulations were performed using the CHARMM36[23] force field for the protein, ADP, K^+, Cl^-, and Mg^{2+}, with the exception of the simulations in which we used an optimized force field for magnesium (referred to as the $Mg_{(ANV)}^{2+}$),[24] and four simulations performed with reduced magnesium of charge of 1.5. Water molecules were modeled using the TIP3P force field.[25] For the phosphate we used $H_2PO_4^-$, which is the protonation state for the phosphate at neutral pH in low ionic-strength solutions,[26] and it has been used as a product in a quantum-mechanical simulation of myosin-catalyzed ATP hydrolysis.[27,28] Moreover, it was proposed that $H_2PO_4^-$ is the form of P_i during release,[29] which is in agreement with simulations showing that a singly protonated phosphate is expelled more rapidly than HPO_4^{2-}, a result obtained in the simulations of actin[30] and F1 ATPase.[16] To generate the force field parameters for $H_2PO_4^-$, we used CGenFF.[31,32] The motor protein was solvated in a box of water using VMD,[33] leaving $\gtrsim$1.5 nm between the protein and each side of the box. The system was neutralized by 2 atoms of K^+, and $\approx$100 K^+ and Cl^- (corresponding to $\approx$0.15 M of KCl) were also added to approximately mimic the cytosolic salinity. The size of the box, number of water molecules, and of ions vary slightly in the different simulations.

Energy Minimization and Equilibration. Before and after solvation, the energy of the system was minimized using NAMD[34] by fixing the position of all the atoms solved by X-ray with the exception of the oxygens of P_i. After the second round of minimization, we performed a short pre-equilibration of 100 ps in which the temperature was slowly raised from 0 K to $\approx$300 K. This equilibration, as well as the rest of the simulations, was performed by restraining the position of the α-carbons of the residues V643−N652 to avoid rigid body motion of the protein. The tethering potential is harmonic, with spring constant 1 kcal/(mol Å^2). Residues V643−N652 constitute part of a helix in the core of the motor, which does not change if the structures of PrePS, P_iR, and nucleotide-free states are superposed. For this reason, these residues were chosen as they are likely not involved in large structural changes during the power stroke (see Figure S1). After the initial, short equilibration, we ran another equilibration for 7.5 ns at a constant pressure (1 Atm) and temperature (300 K). To get consistent results, the last part of the equilibration was always performed using NAMD 2.11 or 2.12, although previous steps of the equilibration were performed using earlier versions of NAMD (2.10) for setup RA-1 (see Table S1). Overall, we found that there is good agreement between the energy and volume sampled during the pressure equilibration performed with NAMD and during the Anton 2 simulations. We excluded from the analysis a few previous simulations performed with Anton (3) and Anton 2 (2) in which the energy, pressure, and volume of the box obtained during equilibration did not match the values reported during sampling. This was a cautious choice because the observables monitored in the excluded simulations did not show any appreciable difference from those discussed here. Unless specified otherwise, the equilibrated structures are referred to as the initial structures.

Simulations on Anton 2 and Data Analyses. We carried out simulations on Anton 2. The list of simulations and other technical details are described in the Supporting Information (SI). The equations of motion were integrated with the Multigrator algorithm,[35] the temperature used is 300 K, and the pressure 1 Atm. The standard settings were employed to perform the simulations. The energy, pressure, and volume were kept constant (within fluctuations) throughout the system. The extended energy (E_X) associate underwent a drift. We compared $\Delta E_X = |E_X(t) - E_X(0)|/|E_X(0)|$ with the results from ref 35. We found that ΔE_X was about twice the value from ref 35 if a time step of 2.5 fs was used, and about 10-times smaller if the time step was 2 fs. Hence, in most simulations, we used 2 fs as a time step. Multiple trajectories (see Table 1 in the SI) using the same initial structures were generated using a different set of initial velocities. For data analyses, we considered only conformations that are 24 ns away from each other. A finer temporal resolution is taken into account exclusively to monitor the trajectory of phosphate release. The data analysis was carried out with VMD,[33] PyMol,[36] MatPlotLib,[37] and a Jupyter notebook.[38]

RESULTS

Analysis of the Initial Structure. In Figure 2a, we show the first coordination shell of magnesium in the crystal structure. Two water molecules, an oxygen from ADP β-phosphate, and P_i coordinate Mg^{2+} together with the side chains of T158 and S204 (we use one letter code for amino acids). The same first coordination shell of Mg^{2+} is found after the initial relaxation from the CA conformation (Figure 2b). The use of an optimized force field for magnesium[24] ($Mg_{(ANV)}^{2+}$) did not change this observation (see Figure 2c). In agreement with quantum mechanical simulations,[27] one hydroxyl group of P_i is directed toward the β phosphate of ADP, and the other is in contact with the side chain of S203. According to a more recent study in myosin,[28] the hydroxyl group of P_i close to the β phosphate is stabilized by a hydrogen bond with the side chain of a serine in the P-loop (S153 in MVI). In the 4PFP structure (and choosing conformation A of 4PJM), the side chain of S153 is close to the hydroxyl group of P_i, which in turn is in proximity to S203. In our case, the hydroxyl group of the side chain of S153 points away from the phosphate due to the choice of one of the alternative conformations (B) present in the crystal structure. The presence of this hydrogen bond might provide additional stabilization of P_i in the binding pocket. Thus, it is possible that its absence might help the release of P_i.

After a short relaxation of the initial RA structure, the nucleotide binding pocket is distorted: an oxygen from ADP α-phosphate and one from ADP β-phosphate have replaced P_i and S204 in the first coordination shell of Mg^{2+} (see Figure 2d). It is reasonable to suggest that this conformational change weakens the interaction between the anion (P_i) and the cation (Mg^{2+}).

https://dx.doi.org/10.1021/acs.jpcb.0c10004
J. Phys. Chem. B 2021, 125, 1107−1117

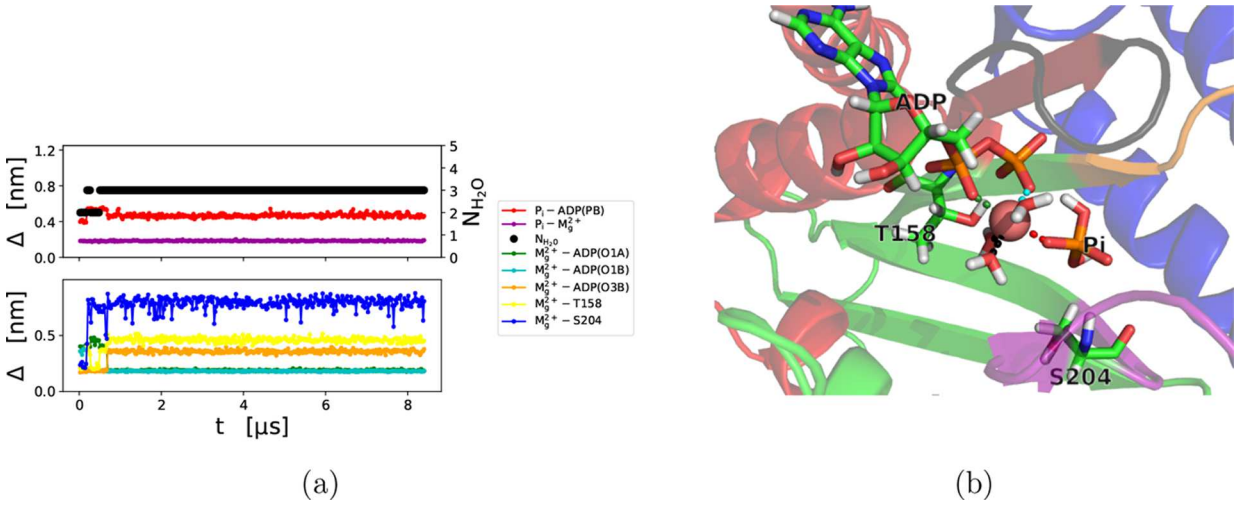

Figure 3. Conformation of the nucleotide binding site during a simulation carried out from the CA initial conformation with the CHARMM energy function. (a) Time-dependent distances of atoms engaged in the first solvation shell of Mg^{2+}. The color code is given in the legend. Red indicates the distance between the β phosphorus of ADP and P_i. The distance between the oxygen of ADP α (β) phosphate and Mg^{2+} is in green (light blue and orange). The contacts between the side chains of the residues T158 and S204 with Mg^{2+} are shown in yellow and blue, respectively. The purple line shows the distance between Mg^{2+} and the oxygen of P_i, which is closest to the cation. Finally, the black dots indicate the number of water molecules in the first shell of Mg^{2+}, computed by counting the number of water oxygens within 2.75 Å from Mg^{2+}. The x-axis shows time in μs, the left y-axis the distance in nm, and the right y-axis the number of water molecules in the first solvation shell of Mg^{2+}. (b) Conformation of the nucleotide binding site after approximately 2.4 μs.

Coordination of Mg^{2+} and P_i Release: Simulations Starting from CA Conformation. In all the simulations beginning from the CA conformation, regardless of the force field used for Mg^{2+}, we do not observe P_i release on the time scales of the simulations, which are several microseconds (see Figures 3a, S2, and S3). By comparing Figures 2b and 3b, it is clear that, given enough time, the side chains of T158 and S204 are replaced in the Mg^{2+} coordination shell by an oxygen of the ADP and an extra water molecule. As shown in Figure 3a (Figures S2 and S3), this exchange occurs within the first microsecond and it remains stable for the rest of the simulation. In most trajectories, three water molecules hydrate Mg^{2+}. In one simulation, carried out using $Mg_{(ANV)}^{2+}$, four water molecules surround the cation for short time intervals, before the hydration observed in the crystal structure is restored, thus preventing P_i release. Notably, lowering the charge of the magnesium to 1.5 did not result in the expulsion of P_i within a few microseconds (see Figure S5).

Coordination of Mg^{2+} and P_i Release: Simulations Starting from the RA Conformation. The P_i is released in 6 out of the 10 simulations generated starting from the RA initial condition. Remarkably, in all of these trajectories, the escape of P_i from the nucleotide binding site occurs only after a fourth water molecule occupies the first solvation shell of Mg^{2+} (see Figure 4 and Figure S4), normally displacing an oxygen of ADP diphosphate group, and in one case the side chain of T158. Note that in one trajectory the P_i re-enters the nucleotide binding site toward the end of the run. In all the other simulations, once the phosphate is released it remains solvated (see Figure S4). These observations allow us to dissect the pathways of P_i release, which we discuss further.

In one simulation (see Figure S4h), the binding of a fourth water molecule to Mg^{2+} does not induce the release of phosphate and it is followed by the rotation of P_i to the CA conformation with three water molecules in the first coordination shell of the cation. This indicates that (i) the arrival of the fourth water molecule is not sufficient to induce the expulsion of the phosphate, even in the RA conformation; (ii) the arrival of the fourth water molecule is reversible; (iii) it is possible to undergo a RA → CA transition. Finally, we also report a RA → CA transition during the equilibration phase of a simulation set up in the RA conformation with the ANV magnesium.

Four Different Exit Pathways. We identified four channels through which the P_i can be released. In two trajectories, the phosphate leaves from the expected back door pathway (purple circle in Figure 5), although it can also escape through the top (red circles in Figure 5) or side route (orange circle in Figure 5). Finally, in one case, the phosphate leaves through the front channel, nearby the ADP (highlighted by a light-blue circle in Figure 5). We examined also the location of P_i during the escape (Figure 6a,b) and compared it with (i) the position of the phosphate during the trajectories that show the release but before the fourth water molecule hydrates Mg^{2+} (Figure 6c), and (ii) with the simulations initiated in the CA conformation (Figure 6d,e). Before the release, P_i is confined in the vicinity of ADP, though in one trajectory we found that the position is distorted and the phosphate moves close to the front exit channel (Figure 6d). On the other hand, during the escape, P_i predominantly populates the expected pathway (Figure 6a,b), in agreement with the crystal structures of myosin VI in the PiR state after they were soaked in a solution containing large quantities of phosphate,[6] which shows two P_i, one by the exit of the tunnel and another in the N-terminal subdomain.

Flexibility of the Converter and the N-Terminal Domain. The converter in myosin VI is pliant: in most trajectories, regardless of the setup, it fluctuates away from the crystal-structure pose (see Figure S7) without significantly changing its conformation (see lower plot in each panel of Figure S7). We also note that the converter in the simulations initiated with the rotated P_i seemed to move the converter earlier than those with the phosphate in the correct orientation. This might suggest some communication between

https://dx.doi.org/10.1021/acs.jpcb.0c10004
J. Phys. Chem. B 2021, 125, 1107−1117

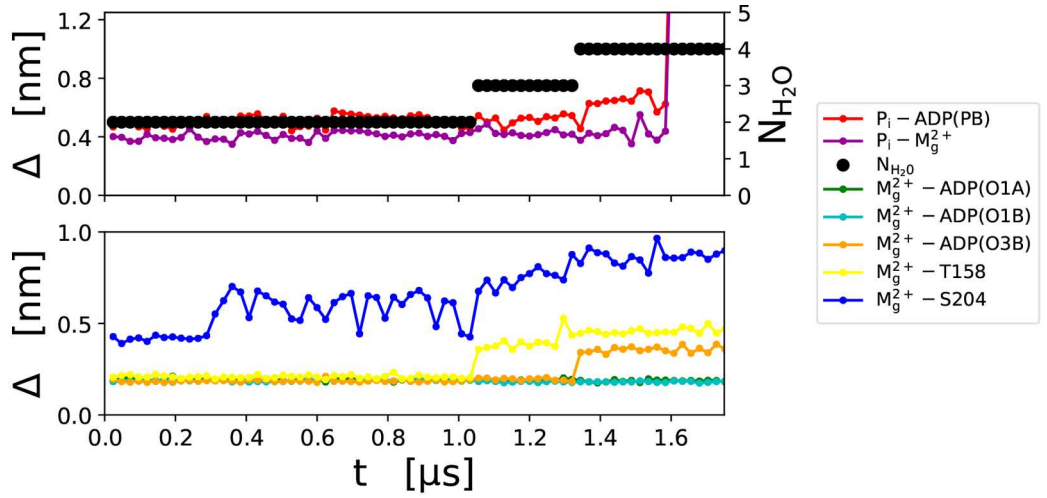

(a)

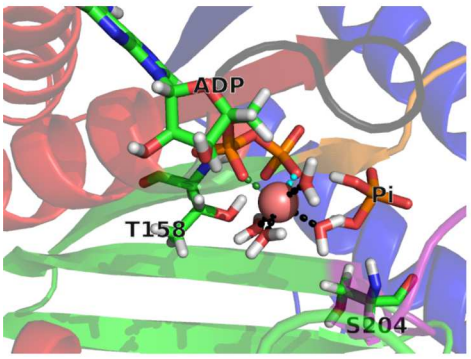

(b)

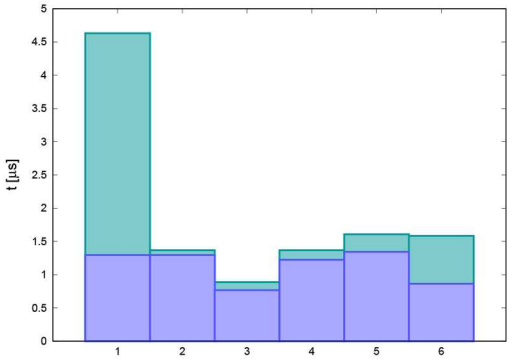

(c)

Figure 4. Conformation of the nucleotide binding site during simulations carried out from the RA initial conformation. (a) Time-dependent distances of atoms engaged in the first solvation shell of Mg^{2+}. The color code (reported in the legend) is the same as in Figure 3a. The trajectory is shown up to the release of phosphate; the entire trajectory is reported in the Supporting Information (see Figure S4g) and shows the re-entry of the phosphate. (b) Conformation of the nucleotide binding site after approximately 1.3 μs, when the fourth water molecule joins the first coordination shell of Mg^{2+}. (c) Time for the stable arrival of the fourth water (blue) and for release of the phosphate (green). The conformations are sampled with a time resolution of 24 ns.

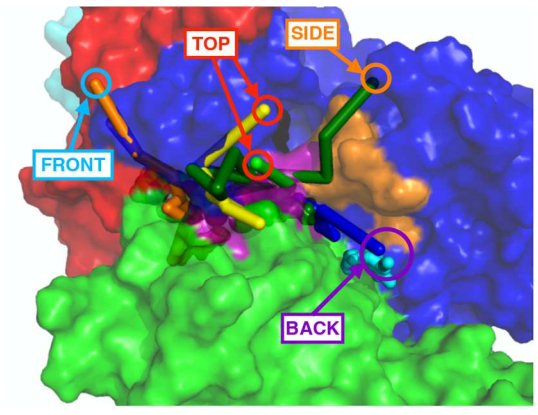

Figure 5. Trajectories of P_i release. Two trajectories are released from the back door (see purple circle). In the red and orange circles are highlighted the trajectories that are released from the top or the side of the back door pathway, respectively. The only trajectory released from the front path, by the ADP, is highlighted with a cyan circle.

the nucleotide binding site and the converter. Surprisingly, we found that in a few simulations the N-terminal β-barrel (NTBB) is mobile (see Figure S8). As for the converter, the structure of the NTBB does not change significantly (see lower plot of each panel in Figure S8), but the whole system detaches from the motor domain and in some cases finds its position close to the converter.

Movement of the ADP. We monitor the conformation of the ADP sugar as the distance between a nitrogen of ADP (N6) and the α carbon of residue N98. As shown in Figure S9, ADP flips out of the pocket more commonly when we start with the rotated P_i and while the phosphate is still bound. Strikingly, after the P_i has left the pocket, the ADP nucleoside maintains its contact with the protein, thus indicating that the rotated P_i might introduce some "stress" in the binding pocket. In the simulations starting with the CA conformation, we rarely see that the ADP sugar flips out of the pocket.

DISCUSSION

Water Triggers Escape of P_i and Prepares ADP for Release. As illustrated in Figures 4, 6, and S4, the phosphate

https://dx.doi.org/10.1021/acs.jpcb.0c10004
J. Phys. Chem. B 2021, 125, 1107−1117

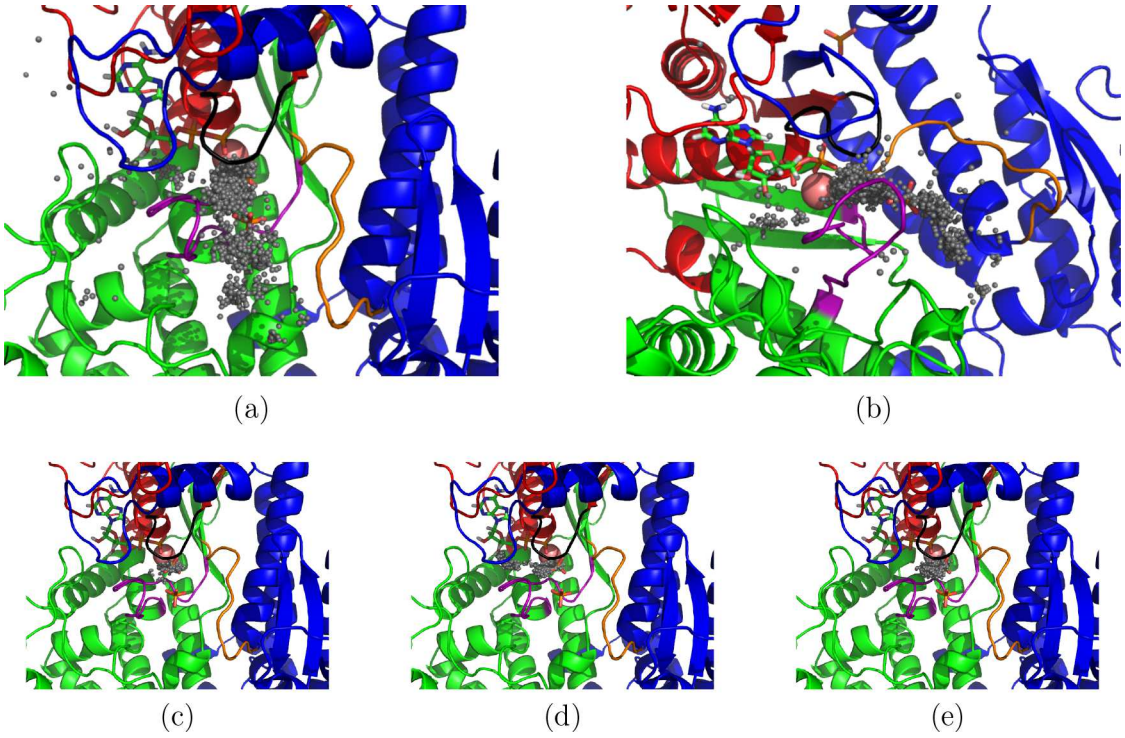

Figure 6. Location of P_i. The gray dots indicate the position of the phosphorus atom of P_i. The conformations sampled during the different trajectories were aligned to a reference structure, of which we report the protein (cartoon), ADP (sticks), and Mg^{2+} (red sphere). We report as sticks also the location of the P_i identified in structure 4PFP and after short soaking of the crystal in a phosphate bath (4PJN),[6] which shows P_i at the exit of the tunnel and in another location in the L-50 domain. (a, b) Trajectories during the last ≈120 ns before the release of P_i, showing only conformations during which four water molecules are bound to the cation. The different points shown are taken from the six trajectories showing the release of P_i at time resolution of 240 ps. The time for the escape was identified from the first frame showing the distance between the phosphorus of P_i and the β phosphorus of ADP exceeded 1.5 nm with a resolution of one frame per 24 ns. Panel a is a top view; the perspective from a side is shown in panel b. (c) Location of P_i during the trajectories starting in the RA conformation showing phosphate release, but with three molecules bound to Mg^{2+}, therefore before the escape of phosphate. Points are sampled at a time resolution of 24 ns. (d, e) Position of the phosphate during the simulations begun in the CA conformation and carried out using (d) CHARMM Mg^{2+} or (e) $Mg_{(ANV)}^{2+}$; time resolution: 24 ns.

does not move away from Mg^{2+} ADP until four water molecule hydrate the cation. This is the major finding of our simulations. It is reasonable that the arrival of a fourth water molecule may weaken the interaction between the cation (Mg^{2+}) and the anion (P_i) by screening the electrostatic attraction and by sterically obstructing the position of the phosphate. In addition, indirect effects could also play a role. For instance, the arrival of the fourth water molecule in the coordination shell of Mg^{2+} requires rearrangement of the ADP diphosphate group, which may in turn affect the interaction with P_i.

In some trajectories, there is a long waiting time between the arrival of the fourth water molecule and the release of phosphate (see Figures 4a and S4). We also observed instances in which a transitory four-water-molecule hydration of P_i does not lead to the escape of phosphate, or trajectories in which P_i is mobile although only three water molecules bind the cation. This indicates that other interactions, which may not be directly affected by the hydration of magnesium, contribute to holding the phosphate in the vicinity of ADP. Therefore, the hydration of magnesium appears to be a necessary but may not be sufficient for phosphate release. Nevertheless, our findings show that the if four water molecules are coordinated to Mg^{2+} release of P_i occurs with high probability.

After the escape of phosphate, the first coordination shell of magnesium remains occupied by four water molecule and two oxygens from ADP. This is likely to weaken the binding between the protein and ADP. We surmise that not only the hydration of Mg^{2+} triggers the escape of phosphate, but it also prepares the release of the nucleotide. The catalytic cycle cannot be completed until these events take place. We note that actin-binding was shown to weaken the interaction between myosin and ADP by favoring a conformation in which ADP release occurs more readily.[39] Hannemann et al.[39] further suggest that the actin-stabilized myosin conformation, which binds ADP weakly and is populated during the hydrolysis cycle, may be induced by the disruption of the coordination shell of Mg^{2+} and may be associated with the escape of P_i. As the PiR structure is supposed to be stabilized by actin, the changes in hydration of the cation, expulsion of P_i, and possibly weakening of ADP binding are in agreement with these experimental observations. However, we have no evidence that magnesium is more weakly bound to the complex, which is also reported by Hannemann et al.[39]

Rotation of Phosphate in the Binding Site. Studies of ATP hydrolysis-induced oxygen exchange showed that the ATP hydrolysis reaction is reversible in myosin,[40−42] including the processive myosin V.[43] As a consequence, if the γ phosphate of ATP is prepared with 3 isotopically labeled oxygens, after repeated cycles of myosin-catalyzed ATP hydrolysis, multiple phosphate oxygens could be exchanged with water, which would reduce the number of labeled oxygens bound to phosphate. Using a quenched-flow setup, it was

https://dx.doi.org/10.1021/acs.jpcb.0c10004
J. Phys. Chem. B 2021, 125, 1107−1117

shown[42] that the kinetics of oxygen exchange is well-described by a model in which all the oxygens of the phosphate are treated identically. The model also implies that the phosphate rotates in the binding pocket on a time scale faster than the competing rates (ATP synthesis and phosphate release). The presence of actin results in a reduced oxygen exchange, which is likely due to the increased rate of phosphate release in the presence of actin,[42] a feature that could be justified if actin stabilizes the formation of the PiR structure. Nevertheless, oxygen exchange is reported in the presence of actin as well. To our knowledge, the extent to which these observations hold for all myosins (and myosin VI in particular) is yet to be fully established. However, there is an indication that over sufficiently long time scales the phosphate rotates in the binding pocket and all of the oxygens behave identically. This suggests that our RA conformation could be not only an expedient to accelerate the release of phosphate but also a short-lived intermediate preceding the escape of P_i.

Taking these studies into consideration, we propose the following model for phosphate release. After hydrolysis, the phosphate rotates in the nucleotide binding site and transitorily orients itself in a RA conformation; then the magnesium is hydrated with four water molecules, which leads to the release of the anion (see Scheme 1). We did not observe

Scheme 1. Phosphate Release Mechanism in Which the Rotation of the Phosphate Is Rate Limiting[a]

$$\mathrm{ADP{\cdot}M_g^{2+}{\cdot}2H_2O{\cdot}(P_i)_{CA}} \overset{\text{rotation}}{\rightleftarrows} \mathrm{ADP{\cdot}M_g^{2+}{\cdot}2H_2O{\cdot}(P_i)_{RA}} \overset{\text{hydration}}{\rightleftarrows} \mathrm{ADP{\cdot}M_g^{2+}{\cdot}4H_2O{\cdot}(P_i)_{RA}} \overset{\text{release}}{\rightleftarrows} \mathrm{ADP{\cdot}M_g^{2+}{\cdot}4H_2O} + P_i$$

[a]Note that the simulations indicate that the speculated CA → RA transition and the observed hydration of magnesium are reversible.

a CA → RA transition during our simulations; however, we report two RA → CA transitions, one of which is concomitant with the reduction of the number of water molecules bound to magnesium from 4 to 3 (see Figure S4h). This indicates that the CA → RA transition may be possible, although because we never observe it, we conclude that (i) it is slower than the simulation time-scale, and (ii) RA is metastable compared to CA. Importantly, though, in the most interesting of the RA → CA transition, the rotation of the phosphate is associated with the loss of one water molecule in the coordination shell of magnesium: if the reverse transition does occur on longer time scales, it may be paired with the hydration of the cation.

Nevertheless, it is possible that the hydration of magnesium occurs in the CA conformation as well, which means that the RA conformation is not a necessary intermediate. This second case is shown in Scheme 2. In Scheme 1, attaining the RA conformation is the bottleneck for phosphate release; in Scheme 2, the hydration of the cation could be the slow process. Overall, whether the RA conformation is an intermediate facilitating P_i escape remains a conjecture that needs to be experimentally tested.

Scheme 2. Phosphate Release Mechanism in Which the Reversible Hydration of the Phosphate Is Rate Limiting[a]

$$\mathrm{ADP{\cdot}M_g^{2+}{\cdot}2H_2O{\cdot}(P_i)_{CA}} \overset{\text{hydration}}{\rightleftarrows} \mathrm{ADP{\cdot}M_g^{2+}{\cdot}4H_2O{\cdot}(P_i)_{CA}} \overset{\text{release}}{\rightarrow} \mathrm{ADP{\cdot}M_g^{2+}{\cdot}4H_2O} + P_i$$

[a]In this scenario, the RA conformation is not an intermediate.

Escape Pathways Are Heterogeneous. Our simulations suggest that, although during release the P_i populates predominantly the "back door" pathway, the escape may occur through multiple gateways. The presence of multiple exit pathways was previously suggested using simulations based on the locally-enhanced sampling (LES) method.[12] Compared to straightforward simulations, LES and other enhanced sampling techniques[16] have the advantage of providing information about the probability of escaping through different channels. On the other hand, our direct simulation protocol enabled us to propose the hydration of the Mg^{2+} as a step of phosphate release; such an insight is most readily obtained via straightforward simulations.

Assessment of Force Field for Mg^{2+}. We ran simulations with two types of Mg^{2+}: (i) from the CHARMM36 force field (Figure S2), (ii) from an improved parametrization[24] (Figure S3). When initializing the simulations in the CA conformation, we did not see the release of phosphate on the time-scale of several μs. The initial structures of the nucleotide binding site obtained with the CHARMM36 Mg^{2+} and with $Mg_{(ANV)}^{2+}$ are similar, and are close to the crystal structure. In both cases though, in a few hundreds of nanoseconds, the interactions between T158 and S204 and Mg^{2+} are lost and a new conformation is found in which more oxygens of ADP are in the first solvation shell of the cation. The rupture of these interactions is not observed in the crystal structures resolved so far, and the new stationary state of the nucleotide binding site deviates from the conformation found in the crystal structure. Although this could be a novel conformation that follows the escape of Pi and prepares the release of ADP, it is unexpected during the CA simulations in which the expulsion of the anion is not observed. We observed the breakage of the interactions of Mg^{2+} with T158 and S204 also during a simulation performed with the α carbon of all residues (with the exception of T158 and S204) fixed (see Figure S6), indicating that the breakage of these interaction is likely not due to some large conformational change in the nucleotide binding pocket, and it appears to be the steady-state arrangement in the nucleotide binding site, which is influenced by the force field. We note that the development of force fields for divalent cations is an active field of research (see for a recent paper, ref 44); the outcome of these studies should help to increase the accuracy of the models such as the one that we discussed here. Despite potential effects of force fields, we believe that based on physical considerations, experimental findings, and comparisons with other biological machines (see below), the proposed mechanism of phosphate release is robust.

Overall Structure of the Motor. Overall, the structure of the motor is intact throughout the simulations. However, as we discussed, regions such as the converter and the NTBB display a large degree of mobility. A recent experimental and numerical study of myosin VI repriming stroke has documented a high level of flexibility for the converter, which occupies a conformation intermediate between the pre- and post-stroke orientations reported by previous structural investigations.[45] Similarly, starting from the PiR, we find that the converter partially moves toward the post-stroke conformation. More surprising is the mobility of the NTBB. We recorded an unhinged NTBB for simulations starting with both CA and RA initial conformations, thus suggesting that the state of the nucleotide binding site might not be the primary

https://dx.doi.org/10.1021/acs.jpcb.0c10004
J. Phys. Chem. B 2021, 125, 1107−1117

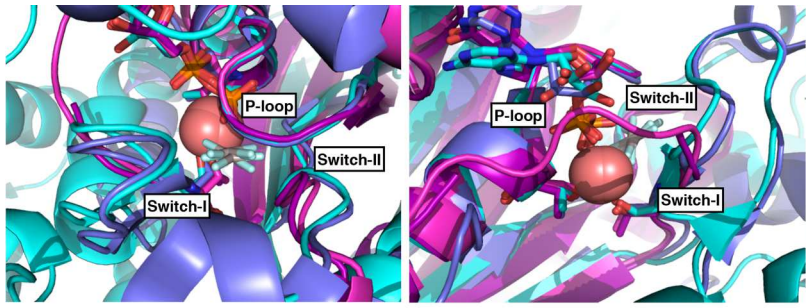

Figure 7. Comparison between the nucleotide binding pockets of molecular motors and G-proteins. In both panels, the cartoon represents myosin (cyan), kinesin (blue), ras-rasGAP (magenta), and rho-rhoGAP (purple). In sticks we show the nucleotide (ADP for motors, GDP for G-proteins) and the ligand AlF_4^- (AlF_3 for ras), which is believed to mimic the transition state (or an intermediate) for hydrolysis. As sticks, we also show two amino acids interacting with Mg^{2+}: T158 (myosin), T92 (kinesin), T19 (rhoA), and S17 (ras) at the end of the P-loop, and S204 (myosin), S202 (kinesin), T37 (rhoA), and T35 (ras) in Switch-I. The red spheres indicate the location of Mg^{2+}. The P-loops of the four proteins were aligned with each other using PyMol.[36] The nucleotides, cation, ligand, and switches nearly superposed. The PDBs used were 4ANJ for myosin,[11] 4HNA for kinesin,[46] whereas for the G-proteins we used 1WQ1 and 1TX4 for ras[47] and rhoA,[48] respectively.

cause of the movement of NTBB. We note that the crystal structure that we used was solved in the presence of glycerol and isopropyl alcohol. In addition, we did not account for the presence of the actin filament. If the PiR structure is indeed stabilized by the interaction with actin, it is possible that some unexpected modes of fluctuations occur in the structure. Finally, some short segments were not solved in the structure and had to be modeled (see Materials and Methods section). Further tests would be necessary to understand the cause and meaning of the large fluctuations of the converter and NTBB domain.

Generality of the Result. The generality of the central result that a 4-fold hydration of Mg^{2+} is necessary for the release of phosphate could be assessed by examining the structures of the nucleotide binding pocket in other systems. Walker et al.[49] observed that many ATPases and GTPases shared common motifs, one of which, denoted as motif A, became known as the P-loop. Once the structures for a series of ATPases and GTPases had been solved, Vale[19] pointed out that G-proteins, myosins, and kinesins are characterized by a similar set of loops around the bound nucleotide, namely the P-loop, Switch-I, and Switch-II. The magnesium ion bound to the nucleotide displays a similar coordination shell, being in contact with a residue (serine or threonine) from the P-loop and Switch-I. In Figure 7, we show the structure of myosin,[11] kinesin,[46] ras,[47] and rhoA[48] in what is believed to be a near transition state conformation for nucleotide hydrolysis: the protein is bound to ADP or GDP, with the phosphate replaced by AlF_4^- or AlF_3. After the structures of the four P-loops were aligned, the location of Switch-I, Switch-II, and the ligands was nearly superposed. In particular, the residues in direct contact with Mg^{2+} show the same position in the binding pocket. In addition, the reversibility of ATP hydrolysis and multiple oxygen exchanges between water and phosphate were reported also for kinesin[50] and rho.[51] With these observations, we surmise that, given the similarity of the binding pocket structure, other ATPases or GTPases may also require the 4-fold hydration of magnesium to release the phosphate. Thus, the occurrence of stepwise hydration of Mg^{2+} could be a prerequisite for phosphate release in a number of machines, which are unrelated by function and share little sequence or structural similarity.

Statistical Significance. Our observation of the release of phosphate is limited to only six events. We excluded some preliminary results that could have provided additional statistics. We discarded these because of some initial setup issues. We did so out of an abundance of caution, as we could not see significant differences in the long-time events that we monitored (see Materials and Methods). The paucity of the number of events warrants a cautionary statement: for instance, we can certainly state that our model indicates that alternative exit pathways exist. However, we cannot ascertain which one is most dominant. Similarly, we cannot exclude, with absolute certainty, that within the context of our model rare events could occur in which the phosphate is ejected without hydration of magnesium, which does seem physically possible. To assess the importance of this mechanism, simulations with the aid of enhanced sampling methods need to performed by fixing the number of water molecules that hydrate the cation and pulling the phosphate outside of the binding pocket. This goes beyond the present manuscript, in which the goal was not to probe the dynamical response of the system along a particular reaction coordinate but to let spontaneous fluctuations guide our understanding of the release mechanism.

■ CONCLUSIONS

Extensive atomic detailed molecular dynamics simulations were used to establish that release of phosphate from the nucleotide binding pocket of a myosin motor occurs only after stepwise hydration of Mg^{2+} by four water molecules. This crucial event occurs in many biological machines and is associated with critical structural transitions. This prompted us to assess if the mechanism of phosphate release is general. On the basis of structural comparisons of nucleotide binding pocket in other machines that bear little relation to the structures or functions of myosin motors, we propose that mechanism for phosphate release is shared among a large class of ATPases and GTPases. This class covers a large number of biological machines. In all the trajectories from which release of phosphate was observed, we discovered that the hydration of the first coordination shell of magnesium by four water molecules precedes the expulsion of P_i. Our finding, which could be universally employed by nature, awaits experimental tests.

https://dx.doi.org/10.1021/acs.jpcb.0c10004
J. Phys. Chem. B 2021, 125, 1107−1117

■ ASSOCIATED CONTENT

Supporting Information

The Supporting Information is available free of charge at https://pubs.acs.org/doi/10.1021/acs.jpcb.0c10004.

List of all simulations; rigid body constraint applied to the system; coordination of magnesium for all trajectories; discussion of movement of converter, N-terminal β-barrel, and ADP for all trajectories (PDF)

■ AUTHOR INFORMATION

Corresponding Author

D. Thirumalai − *Department of Chemistry, The University of Texas at Austin, Austin, Texas 78712, United States;* orcid.org/0000-0003-1801-5924; Email: dave.thirumalai@gmail.com

Author

Mauro Lorenzo Mugnai − *Department of Chemistry, The University of Texas at Austin, Austin, Texas 78712, United States;* orcid.org/0000-0002-0267-2279

Complete contact information is available at: https://pubs.acs.org/10.1021/acs.jpcb.0c10004

Notes

The authors declare no competing financial interest.

■ ACKNOWLEDGMENTS

We thank Prof. Yale E. Goldman and Prof. Enrique M. De La Cruz for referring us to the oxygen exchange experiments, ultrafast force clamp studies, and the interplay between magnesium and ADP in the nucleotide binding pocket. We also thank Dr. D. Chakraborty, Dr. A. Kumar, and Dr. S. Shin for a critical reading of the manuscript. This work was supported in part by the National Science Foundation (CHE 19-00093) and the Collie-Welch Chair administered through the Welch Foundation (F-0019). Anton 2 computer time was provided by the Pittsburgh Supercomputing Center (PSC) through Grant No. R01GM116961 from the National Institutes of Health. The Anton 2 machine at PSC was generously made available by D.E. Shaw Research.

■ DEDICATION

We are pleased to dedicate this paper to Lawrence Pratt whose pioneering works on the unique role of water in chemistry and biology have been a guiding light.

■ REFERENCES

(1) Geeves, M. A.; Holmes, K. C. Structural Mechanism of Muscle Contraction. *Annu. Rev. Biochem.* **1999**, *68*, 687−728.

(2) Sweeney, H. L.; Houdusse, A. Structural and functional insights into the myosin motor mechanism. *Annu. Rev. Biophys.* **2010**, *39*, 539−557.

(3) De La Cruz, E. M.; Ostap, E. M.; Sweeney, H. L. Kinetic mechanism and regulation of myosin VI. *J. Biol. Chem.* **2001**, *276*, 32373−32381.

(4) Fisher, A. J.; Smith, C. A.; Thoden, J.; Smith, R.; Sutoh, K.; Holden, H. M.; Rayment, I. X-ray Structures of the Myosin Motor Domain of Dictyostelium discoideum Complexed with MgADP·BeF_x and MgADP·AlF_4^-. *Biochemistry* **1995**, *34*, 8960−8972.

(5) Yount, R. G.; Lawson, D.; Rayment, I. Is myosin a "back door" enzyme? *Biophys. J.* **1995**, *68*, 44S.

(6) Llinas, P.; Isabet, T.; Song, L.; Ropars, V.; Zong, B.; Benisty, H.; Sirigu, S.; Morris, C.; Kikuti, C.; Safer, D.; Sweeney, H.; Houdusse, A. How Actin Initiates the Motor Activity of Myosin. *Dev. Cell* **2015**, *33*, 401−412.

(7) Sellers, J. R.; Veigel, C. Direct observation of the myosin-Va power stroke and its reversal. *Nat. Struct. Mol. Biol.* **2010**, *17*, 590−595.

(8) Dantzig, J.; Goldman, Y.; Millar, N.; Lacktis, J.; Homsher, E. Reversal of the cross-bridge force-generating transition by photogeneration of phosphate in rabbit psoas muscle fibres. *J. Physiol.* **1992**, *451*, 247−278.

(9) Woody, M.; Capitanio, M.; Winkelmann, D.; Ostap, E. M.; Goldman, Y. E. Single molecule mechanics resolves the earliest events in force generation by cardiac myosin. *eLife* **2019**, *8*, e49266.

(10) Gurel, P. S.; Kim, L. Y.; Ruijgrok, P. V.; Omabegho, T.; Bryant, Z.; Alushin, G. M. Cryo-EM structures reveal specialization at the myosin VI-actin interface and a mechanism of force sensitivity. *eLife* **2017**, *6*, e31125.

(11) Ménétrey, J.; Isabet, T.; Ropars, V.; Mukherjea, M.; Pylypenko, O.; Liu, X.; Perez, J.; Vachette, P.; Sweeney, H. L.; Houdusse, A. M. Processive steps in the reverse direction require uncoupling of the lead head lever arm of myosin VI. *Mol. Cell* **2012**, *48*, 75−86.

(12) Cecchini, M.; Alexeev, Y.; Karplus, M. Pi release from myosin: a simulation analysis of possible pathways. *Structure* **2010**, *18*, 458−470.

(13) Shaw, D. E.; Grossman, J.; Pram, J. A.; Batson, B.; Butts, J. A.; Chao, J. C.; Deneroff, M. M.; Dror, R. O.; Even, A.; Fenton, C. H.; Forte, A.; Gagliardo, J.; Gill, G.; Greskamp, B.; Ho, C. R.; Ieraldi, D. J.; Iserovich, L.; Kuskin, J. S.; Larson, R. H.; Layman, T.; Lee, L.-S.; Lerer, A. K.; Li, C.; Killebrew, D.; Mackenzie, K. M.; Mok, S. Y.-H.; Moraes, M. A.; Mueller, R.; Nociolo, L. J.; Peticolas, J. L.; Quan, T.; Ramot, D.; Salmon, J. K.; Scarpazza, D. P.; Schafer, N.; Siddique, N.; Snyder, C. W.; Spengler, J.; Tang, P. T. P.; Theobald, M.; Toma, H.; Towles, B.; Vitale, B.; Wang, S. C.; Young, C. Anton 2: raising the bar for performance and programmability in a special-purpose molecular dynamics supercomputer. *Proceedings of the international conference for high performance computing, networking, storage and analysis* **2014**, 41−53.

(14) Sato, O.; White, H. D.; Inoue, A.; Belknap, B.; Ikebe, R.; Ikebe, M. Human deafness mutation of myosin VI (C442Y) accelerates the ADP dissociation rate. *J. Biol. Chem.* **2004**, *279*, 28844−28854.

(15) Pylypenko, O.; Song, L.; Shima, A.; Yang, Z.; Houdusse, A. M.; Sweeney, H. L. Myosin VI deafness mutation prevents the initiation of processive runs on actin. *Proc. Natl. Acad. Sci. U. S. A.* **2015**, *112*, E1201−E1209.

(16) Okazaki, K.-i.; Hummer, G. Phosphate release coupled to rotary motion of F1-ATPase. *Proc. Natl. Acad. Sci. U. S. A.* **2013**, *110*, 16468−16473.

(17) Hyeon, C.; Thirumalai, D. Capturing the essence of folding and functions of biomolecules using coarse-grained models. *Nat. Commun.* **2011**, *2*, 487.

(18) Elber, R.; West, A. Atomically detailed simulation of the recovery stroke in myosin by Milestoning. *Proc. Natl. Acad. Sci. U. S. A.* **2010**, *107*, 5001−5005.

(19) Vale, R. D. Switches, latches, and amplifiers: common themes of G proteins and molecular motors. *J. Cell Biol.* **1996**, *135*, 291−302.

(20) Guex, N.; Peitsch, M. C. SWISS-MODEL and the Swiss-Pdb Viewer: an environment for comparative protein modeling. *Electrophoresis* **1997**, *18*, 2714−2723.

(21) Søndergaard, C. R.; Olsson, M. H.; Rostkowski, M.; Jensen, J. H. Improved treatment of ligands and coupling effects in empirical calculation and rationalization of pKa values. *J. Chem. Theory Comput.* **2011**, *7*, 2284−2295.

(22) Olsson, M. H.; Søndergaard, C. R.; Rostkowski, M.; Jensen, J. H. PROPKA3: consistent treatment of internal and surface residues in empirical pKa predictions. *J. Chem. Theory Comput.* **2011**, *7*, 525−537.

(23) Vanommeslaeghe, K.; Hatcher, E.; Acharya, C.; Kundu, S.; Zhong, S.; Shim, J.; Darian, E.; Guvench, O.; Lopes, P.; Vorobyov, I.; Mackerell, A. D. CHARMM general force field: A force field for drug-like molecules compatible with the CHARMM all-atom additive biological force fields. *J. Comput. Chem.* **2009**, *31*, 671−NA.

(24) Allnér, O.; Nilsson, L.; Villa, A. Magnesium ion−water coordination and exchange in biomolecular simulations. *J. Chem. Theory Comput.* **2012**, *8*, 1493−1502.
(25) Jorgensen, W. L.; Chandrasekhar, J.; Madura, J. D.; Impey, R. W.; Klein, M. L. Comparison of simple potential functions for simulating liquid water. *J. Chem. Phys.* **1983**, *79*, 926−935.
(26) Powell, K. J.; Brown, P. L.; Byrne, R. H.; Gajda, T.; Hefter, G.; Sjöberg, S.; Wanner, H. Chemical speciation of environmentally significant heavy metals with inorganic ligands. Part 1: The Hg2+− Cl−, OH−, CO32−, SO42−, and PO43−aqueous systems (IUPAC Technical Report). *Pure Appl. Chem.* **2005**, *77*, 739−800.
(27) Schwarzl, S. M.; Smith, J. C.; Fischer, S. Insights into the chemomechanical coupling of the myosin motor from simulation of its ATP hydrolysis mechanism. *Biochemistry* **2006**, *45*, 5830−5847.
(28) Kiani, F. A.; Fischer, S. Catalytic strategy used by the myosin motor to hydrolyze ATP. *Proc. Natl. Acad. Sci. U. S. A.* **2014**, *111*, 201401862.
(29) Grigorenko, B. L.; Rogov, A. V.; Topol, I. A.; Burt, S. K.; Martinez, H. M.; Nemukhin, A. V. Mechanism of the myosin catalyzed hydrolysis of ATP as rationalized by molecular modeling. *Proc. Natl. Acad. Sci. U. S. A.* **2007**, *104*, 7057−7061.
(30) Wriggers, W.; Schulten, K. Investigating a back door mechanism of actin phosphate release by steered molecular dynamics. *Proteins: Struct., Funct., Genet.* **1999**, *35*, 262−273.
(31) Vanommeslaeghe, K.; MacKerell, A. D., Jr. Automation of the CHARMM General Force Field (CGenFF) I: bond perception and atom typing. *J. Chem. Inf. Model.* **2012**, *52*, 3144−3154.
(32) Vanommeslaeghe, K.; Raman, E. P.; MacKerell, A. D., Jr. Automation of the CHARMM General Force Field (CGenFF) II: Assignment of Bonded Parameters and Partial Atomic Charges. *J. Chem. Inf. Model.* **2012**, *52*, 3155−3168.
(33) Humphrey, W.; Dalke, A.; Schulten, K. VMD: visual molecular dynamics. *J. Mol. Graphics* **1996**, *14*, 33−38.
(34) Phillips, J. C.; Braun, R.; Wang, W.; Gumbart, J.; Tajkhorshid, E.; Villa, E.; Chipot, C.; Skeel, R. D.; Kale, L.; Schulten, K. Scalable molecular dynamics with NAMD. *J. Comput. Chem.* **2005**, *26*, 1781−1802.
(35) Lippert, R. A.; Predescu, C.; Ierardi, D. J.; Mackenzie, K. M.; Eastwood, M. P.; Dror, R. O.; Shaw, D. E. Accurate and efficient integration for molecular dynamics simulations at constant temperature and pressure. *J. Chem. Phys.* **2013**, *139*, 164106.
(36) *The PyMOL Molecular Graphics System, Version 1.7.6.0*; Schrödinger, LLC, 2015.
(37) Hunter, J. D. Matplotlib: A 2D Graphics Environment. *Comput. Sci. Eng.* **2007**, *9*, 90−95.
(38) Kluyver, T.; Ragan-Kelley, B.; Pérez, F.; Granger, B.; Bussonnier, M.; Frederic, J.; Kelley, K.; Hamrick, J.; Grout, J.; Corlay, S.; Ivanov, P.; Avila, D.; Abdalla, S.; Willing, C. Jupyter Development Team, Jupyter Notebooks-a publishing format for reproducible computational workflows. *ELPUB* **2016**, 87−90.
(39) Hannemann, D. E.; Cao, W.; Olivares, A. O.; Robblee, J. P.; De La Cruz, E. M. Magnesium, ADP, and Actin Binding Linkage of Myosin V: Evidence for Multiple Myosin V- ADP and Actomyosin V-ADP States. *Biochemistry* **2005**, *44*, 8826−8840.
(40) Bagshaw, C.; Trentham, D. The reversibility of adenosine triphosphate cleavage by myosin. *Biochem. J.* **1973**, *133*, 323−328.
(41) Geeves, M. A.; Webb, M. R.; Midelfort, C. F.; Trentham, D. R. Mechanism of adenosine 5′-triphosphate cleavage by myosin: studies with oxygen-18-labeled adenosine 5′-triphosphate. *Biochemistry* **1980**, *19*, 4748−4754.
(42) Webb, M. R.; Trentham, D. R. The mechanism of ATP hydrolysis catalyzed by myosin and actomyosin, using rapid reaction techniques to study oxygen exchange. *J. Biol. Chem.* **1981**, *256*, 10910−10916.
(43) Olivares, A. O.; Chang, W.; Mooseker, M. S.; Hackney, D. D.; De La Cruz, E. M. The tail domain of myosin Va modulates actin binding to one head. *J. Biol. Chem.* **2006**, *281*, 31326−31336.
(44) Villa, F.; MacKerell, A. D.; Roux, B.; Simonson, T. Classical Drude Polarizable Force Field Model for Methyl Phosphate and Its Interactions with Mg2+. *J. Phys. Chem. A* **2018**, *122*, 6147.
(45) Blanc, F.; Isabet, T.; Benisty, H.; Sweeney, H. L.; Cecchini, M.; Houdusse, A. An intermediate along the recovery stroke of myosin VI revealed by X-ray crystallography and molecular dynamics. *Proc. Natl. Acad. Sci. U. S. A.* **2018**, *115*, 6213−6218.
(46) Gigant, B.; Wang, W.; Dreier, B.; Jiang, Q.; Pecqueur, L.; Plückthun, A.; Wang, C.; Knossow, M. Structure of a kinesin-tubulin complex and implications for kinesin motility. *Nat. Struct. Mol. Biol.* **2013**, *20*, 1001.
(47) Scheffzek, K.; Ahmadian, M. R.; Kabsch, W.; Wiesmüller, L.; Lautwein, A.; Schmitz, F.; Wittinghofer, A. The Ras-RasGAP complex: structural basis for GTPase activation and its loss in oncogenic Ras mutants. *Science* **1997**, *277*, 333−339.
(48) Rittinger, K.; Walker, P. A.; Eccleston, J. F.; Smerdon, S. J.; Gamblin, S. J. Structure at 1.65 Å of RhoA and its GTPase-activating protein in complex with a transition-state analogue. *Nature* **1997**, *389*, 758.
(49) Walker, J. E.; Saraste, M.; Runswick, M. J.; Gay, N. J. Distantly related sequences in the alpha-and beta-subunits of ATP synthase, myosin, kinases and other ATP-requiring enzymes and a common nucleotide binding fold. *EMBO J.* **1982**, *1*, 945−951.
(50) Hackney, D. D. The tethered motor domain of a kinesin-microtubule complex catalyzes reversible synthesis of bound ATP. *Proc. Natl. Acad. Sci. U. S. A.* **2005**, *102*, 18338−18343.
(51) Phillips, R. A.; Hunter, J. L.; Eccleston, J. F.; Webb, M. R. The mechanism of Ras GTPase activation by neurofibromin. *Biochemistry* **2003**, *42*, 3956−3965.

https://dx.doi.org/10.1021/acs.jpcb.0c10004
J. Phys. Chem. B 2021, 125, 1107−1117